Available online at www.sciencedirect.com
ScienceDirect
Ceramics International 36 (2010) 181–185
CERAMICS INTERNATIONAL
www.elsevier.com/locate/ceramint

Microwave dielectric properties of Mn-doped BaO–$(Nd_{0.7},Sm_{0.3})_2O_3$–$4TiO_2$ ceramic sintered in a reducing atmosphere

Wen-His Lee [a,*], Ying-Chieh Lee [b]

[a] Department of Electrical Engineering, National Cheng Kung University, No. 1 University Road, Tainan, Taiwan
[b] Department of Materials Engineering, National Ping-Tung University of Technology, Taiwan

Received 16 June 2008; received in revised form 15 April 2009; accepted 10 July 2009
Available online 11 August 2009

Abstract

The effect of $MnCO_3$ doped from 0 to 55 mol% into BaO–$(Nd_{0.7}Sm_{0.3})_2O_3$–$4TiO_2$ (BNST) sintered in a reducing atmosphere on the microstructure and electrical properties was studied. Mn^{3+} completely substituted into Ti^{4+}-sites of BNST to form a solid solution, so there is no second phase until 42 mol% which is the maximum solubility. Mn (<42 mol%)-doped BNST sintered in a reducing atmosphere is in a semiconducing state because the concentration of free electron is higher than that of the acceptors. On the other hand, when Mn content doped into BNST exceeds a critical value (>43 mol%), the second Mn-rich phase due to excess of Mn^{3+} substituted into Ti^{4+}-site, corresponding to original BaO–$(Nd_{0.7}Sm_{0.3})_2O_3$–$4TiO_2$ (1 1 4) phase, is formed. Mn (>43 mol%)-doped BNST sintered in a reducing atmosphere is in an insulating state because the concentration of the acceptors is higher than that of liberated free electron, so the insulation resistance becomes high and tan δ becomes low. The formation of the second Mn-rich phase affects $Q \times f$ factor and temperature coefficient of capacitance (T.C.C.) of BNST significantly.

Keywords: A. Sintering; C. Dielectric properties; Ceramic; X-ray diffraction

1. Introduction

Several dielectric materials such as $Ba_{6-3x}RE_{8+2x}Ti_{18}O_{54}$ (where RE = rare earth), $CaZrO_3$, $BaTi_4O_9$, and $Ba_2Ti_9O_{20}$ are typical base compositions for temperature compensation (TC)-type multilayer ceramic capacitors (MLCCs). Usually, these dielectric materials are sintered above 1300 °C in air and electrical properties can meet the NPO (negative–positive–zero) specifications, meaning that the temperature coefficient of capacitance (T.C.C.) is ± 30 ppm/°C, $\tan\delta \leq 0.01\%$ and insulation resistance (I.R.) $\geq 10^{11}\,\Omega$ at 25 °C based on 1.0 mm × 1.00 mm × 0.5 mm dimension. Moreover, among these dielectrics, $Ba_{6-3x}RE_{8+2x}Ti_{18}O_{54}$ based dielectric has attracted much attention from materials scientists because of its excellent dielectric properties particularly because of its high dielectric constant (>80) and microwave properties. Among the RE elements, La, Nd, Sm and Gd are commonly reported. The BaO–$(Nd,Sm)_2O_3$–$4TiO_2$ system contains a 1:1:4 phase ($Ba_{4.5}(Nd,Sm)_9Ti_{18}O_{54}$) with excellent physical properties and is suitable for MLCC application [1–4]. The relative dielectric constant, $\varepsilon_r \sim 85$, T.C.C. (temperature coefficient of capacitance) -113 ppm/°C, and $\tan\delta \sim 0.05\%$ at 1 MHz were reported. τ_ε can be fine tuned to near zero through the addition of dopants such as Sm, Sr, and Pb.

To reduce the production cost of the inner and outer electrode of MLCC, the base metal electrode (BME) such as Ni or Cu is used to replace the noble-metal electrode (NBE) such as Pd or Ag. However, to prevent Cu, or Ni from oxidation, the green bricks have to be sintered in a partially reducing atmosphere (in H_2/N_2 forming gas, $P_{O_2} = 10^{-10}$ to 10^{-12} atm), and then the re-oxidation of bricks is performed in a weak reducing atmosphere in N_2 ($P_{O_2} = 10^{-7}$ to 10^{-9} atm) to compensate for the lack of oxygen in dielectric sintered in a strong reducing atmosphere. A well-known case is that when $BaTiO_3$ with a perovskite structure is fired in a reducing atmosphere, oxygen is lost from the lattice, simultaneously the doubly ionized oxygen vacancies are formed and the free electrons in the conduction band are liberated. Thus, a large number of oxygen vacancies ($V_O^{\bullet\bullet}$) and free electrons (e^-) are generated during sintering in a reducing atmosphere, leading to low insulation resistance and the short long-term reliability test

* Corresponding author. Tel.: +886 6 2757575x62445; fax: +886 2345482.
E-mail address: leewen@mail.ncku.edu.tw (W.-H. Lee).

0272-8842/$36.00
doi:10.1016/j.ceramint.2009.07.006

against high voltage. Therefore, as previously reported [5], the addition of dopants such as Mn^{2+}or Mn^{3+} to $BaTiO_3$ and re-oxidation at an appropriate temperature are two main keys to improve the insulation resistance or long-term reliability test of $BaTiO_3$. Generally, the re-oxidation in a weak reducing atmosphere (in nitrogen) is accompanied by the oxidation of manganese ions to the trivalent state [6], regardless of the valence of the raw materials of manganese. Acceptor ions such as Mn^{3+} on Ti^{4+}-sites give rise to oxygen vacancies but without the liberation of electrons since acceptor ions play a role in shifting the minimum in the conductivity–oxygen pressure relation to lower oxygen pressures. Therefore, the concentration of electrons in the conduction band is reduced and positive holes in the valence band become the majority carries when $BaTiO_3$ is sintered in a reducing atmosphere.

In this study, the base metal, nickel, is conducted to a $Ba_{6-3x}(Nd_{0.7}Sm_{0.3})_{8+2x}Ti_{18}O_{54}$ dielectric as an inner electrode to form MLCC with the negative–positive–zero (NPO) temperature characteristic, meaning that the $Ba_{6-3x}(Nd_{0.7}Sm_{0.3})_{8+2x}Ti_{18}O_{54}$ dielectric has to be sintered in a reducing atmosphere to prevent the Ni-inner electrode from oxidation. However, $Ba_{6-3x}(Nd_{0.7}Sm_{0.3})_{8+2x}Ti_{18}O_{54}$ with a tungsten bronze-type structure sintered in a reducing atmosphere also shows the semi-conducting behavior. A useful dopant, manganese, is used to prevent $BaTiO_3$ from semi-conducting when it was sintered in a reducing atmosphere. Thus, the main objective of this study is to examine the effect of manganese on the microstructure, and electrical properties of $Ba_{6-3x}(Nd_{0.7}Sm_{0.3})_{8+2x}$ $Ti_{18}O_{54}$-based dielectrics sintered in a reducing atmosphere.

2. Experimental procedure

2.1. Preparation of specimens

Powders were synthesized by a solid-state reaction. Reagent-grade $BaCO_3$ (Solvay, Italy), TiO_2 (Fuji Inc. Japan), Nd_2O_3, Sm_2O_3 (H.C. Stack Inc., Japan) and $MnCO_3$ (Showa Chemicals, Japan) with 99.9% purity were weighed based on $BaO–(Nd_{0.7}Sm_{0.3})_2O_3–4TiO_2$ (BNST) formulation, and then dispersed in an ethanol–toluene mixture solvent system, and then milled for 4 h. The powders were calcined at 1150 °C for 4 h in air. After calcinations, the samples were crushed using an agate mortar and milled for 1 h at 200 rpm using a planetary ball-mill using 2 mm yttria-tetragonal zirconia polycrystal (Y-TZP) balls. Usually, $MnCO_3$ from 1 to 55 mol% with respect to the BNST-based powder was then added. The ratio of ethanol to toluene was 1:1 and the solid content of the slurry was 55 wt%. The dispersant used was 1.0 wt% DD34 from Daido chemicals which is a polyacrylic acid, partly neutralized with ammonia and with part of the carboxylic groups having an ester group, the proportion of ester being based on the total amount of powder added to the slurry. After drying overnight, the mixed powders were pulverized, sieved, granulated and die-pressed into a disk of 6 mm in diameter. The green bricks were sintered at 1300 °C for 2 h in a 3% H_2/N_2 atmosphere and re-oxidated at 1000 °C for 3 h in N_2. After firing, the Cu conductive paste was painted onto the surface of the specimens and then cured at 900 °C for 30 min in N_2 to strengthen the adhesion of the Cu terminal electrode with the sintered bodies.

2.2. Phase identification and microstructure analysis

The crystalline phase of the specimens was determined by X-ray diffractometry (XRD) (X'Pert, Philips, Netherlands). The microstructure of the specimens was characterized by scanning electron spectroscopy (JSM-5300, JEOL, Japan) equipped with an energy-dispersive spectrometer (6587, Oxford Instruments, England).

2.3. Measurement of microwave dielectric properties

The dielectric properties including the capacitance and dissipation factor (tan δ) were measured using a precision LCR network analyzer (4284A, Hewlett-Packard Inc., U.S.A.). T.C.C. is the temperature coefficient of capacitance measured at 1 MHz equipped with a thermostat. The insulation resistance (IR) of the samples was measured using a high resistive meter (4339B, Hewlett-Packard Inc., U.S.A.) at an applied voltage of 25 V for 1 s. The $Q \times f_o$ were measured at 4–5 GHz by Hakki and Coleman's resonator method [7].

3. Results and discussion

3.1. Phase identification and microstructure examination

The XRD spectra of 0–26 mol% Mn-doped BNST after sintering at 1300 °C for 2 h in a 3% H_2/N_2 atmosphere and re-oxidation at 1000 °C for 3 h in N_2 are shown in Fig. 1. It is found that the similar XRD spectra can be obtained when doping Mn from 1 up to 26 mol%. All materials show a tungsten bronze-type $Ba_{6-3x}Re_{8+2x}Ti_{18}O_{54}$ solid solutions when the composition corresponds exactly to $x = 0.5$ that has been confirmed by Varfolomeev et al. [8] (please refer to ICDD card No. 43-0235). The results show that no formation of new phase can be found, which imply manganese ion could form a complete solid solution with BNST under this condition. The valence of Mn is changed from divalent to trivalent state after re-oxidation in nitrogen after confirmation by electron spectroscopy for chemical analysis (ESCA). It obviously exhibits a preference for the Ti-sites due to the small difference of atomic radius between Mn^{3+}($R_{[B]} = 0.058$ nm) and Ti^{4+}($R_{[B]} = 0.061$ nm). The maximum solubility of Mn^{3+} in Ti^{4+}-sites of $BaO–(Nd_{0.7}Sm_{0.3})_2O_3–4TiO_2$ is approximately 42 mol%.

Fig. 2 shows the XRD spectra of 43–55 mol% heavily Mn-doped BNST dielectrics. The XRD spectra indicate that the phase change can be found as the addition of Mn content is more than 43 mol%. A splitting of peaks takes place at the angle of 31.6°, corresponding BSTN without Mn doping, but the extra peak is not the Mn_2O_3 phase. The strongest peak 151 of Mn-doped BNST at approximately 31.6° was examined by step scanning at 0.02°/s from 27° to 33°. Fig. 3 shows the change in the strongest peak of BNST as Mn content increases from 7 to 55 mol%. For BNST specimens with 7, 26 and 42 mol% Mn

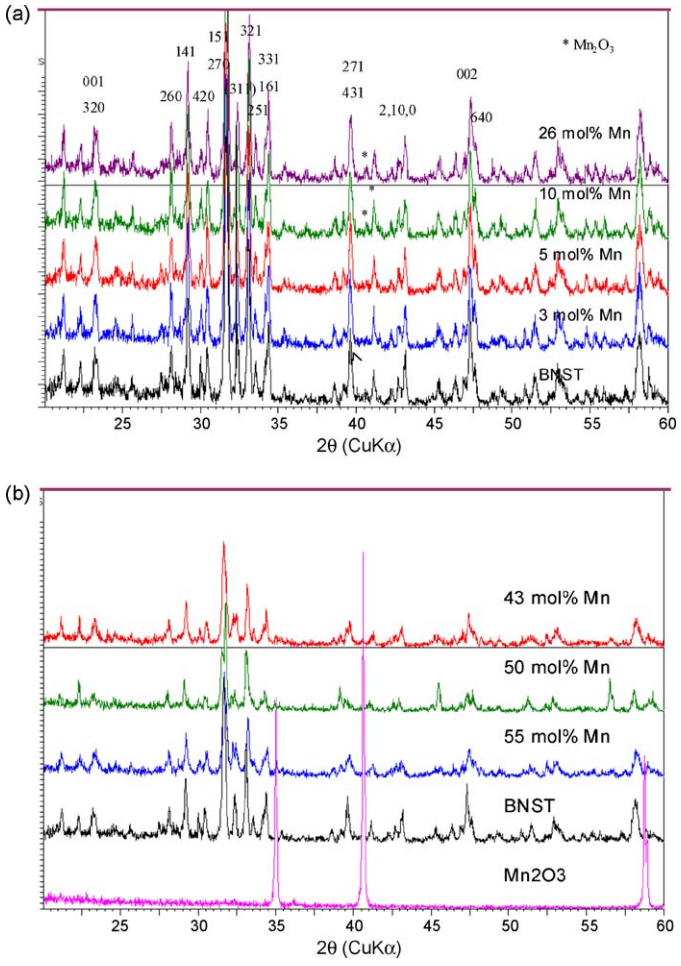

Fig. 1. (a) XRD spectrum for 0, 3, 5, 7, 10 mol% Mn-doped BNST. (b) XRD spectrum for 43, 50, 55 mol% Mn-doped BNST.

doping, the single peak 151 of Mn-doped BNST is observed. However, for heavily Mn-doped BNST specimens with 43, 44 and 45 mol% Mn doping, a shoulder peak at a higher angle than that of the strongest peak 151 is observed. When Mn content is successively increased above 46 mol%, the shoulder peak is changed into an extra peak at 31.8° and the strongest peak

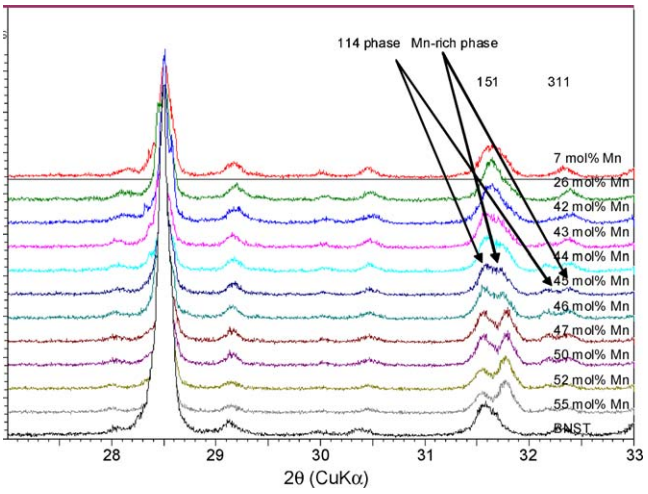

Fig. 2. Step scan for the strongest peak (1 5 1) of 7–55 mol% Mn-doped BNST.

(1 5 1) of BNST is at approximately 31.55°, simultaneously, another peak of (3 1 1) also is split into two peaks. Obviously, there is a formation of the second phase when the amount of Mn was continuously increased more than 43 mol%. The crystalline structure of the Mn-rich second phase is similar to Mn-doped BNST with a tungsten bronze-type structure.

Mn was heavily doped (>43 mol%) into $BaO–(Nd_{0.7}Sm_{0.3})_2O_3–4TiO_2$ to affect the number of formation of phase, this result is associated with the stoichiometry of $BaO–(Nd_{0.7}Sm_{0.3})_2O_3–4TiO_2$. A stoichiometric $BaO–(Nd_{0.7}Sm_{0.3})_2O_3–4TiO_2$ is single phase. However, a non-stoichiometric $BaO–(Nd_{0.7}Sm_{0.3})_2O_3–4TiO_2$ meaning $BaO–(Nd_{0.7}Sm_{0.3})_2O_3–4TiO_2$ with big excess of Mn_2O_3 is in the presence of dual phases including $BaO–(Nd,Sm)_2O_3–4(Ti_{1-2x},Mn_{2x})O_{3-x}$ phase and Mn-rich phase.

Fig. 3 exhibits the SEM micrograph and EDS spectra of 50 mol% Mn-doped BNST dielectrics. The image shows a dual-phase microstructure. One phase is gray phase, which forms a continuous matrix. The other phase consists of dark precipitates, which are dispersed in the matrix. The EDS spectra indicate that the gray phase is a Ti-rich phase that is composed of a $BaO–(Nd,Sm)_2O_3–4(Ti_{1-2x},Mn2_x)O_{3-x}$ phase, while the dark precipitate is a Mn-rich phase.

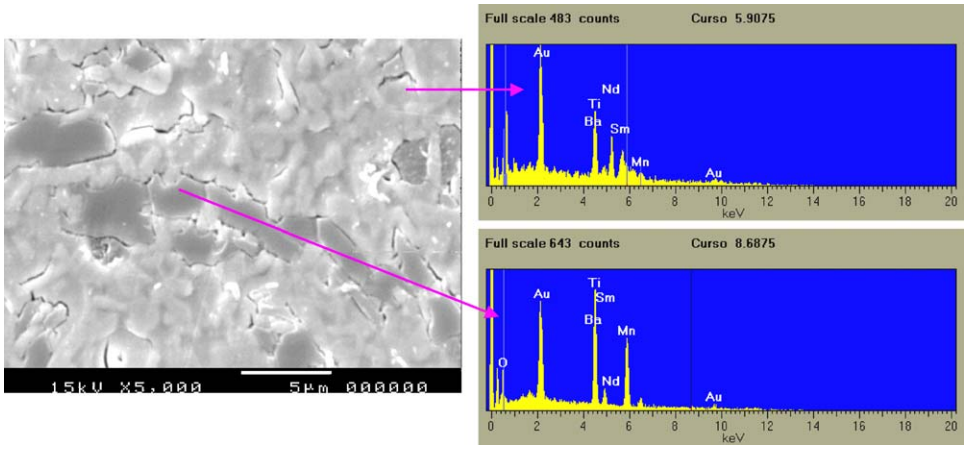

Fig. 3. The fractured SEM micrographs (5000 magnification) and EDS spectrum of 50 mol% Mn-doped BNST.

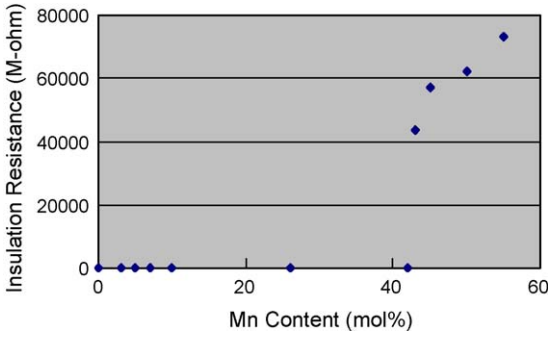

Fig. 4. Variation of insulation resistance as a function of Mn content.

On the basis of these results, the following reactions are proposed when Mn-doped BNST is sintered in a reducing atmosphere.

Regime (I) (Mn: 0–42 mol%)

$$\mathrm{BaO{-}(Nd,Sm)_2O_3{-}4TiO_2 + MnCO_3 \rightarrow BaO{-}(Nd,Sm)_2O_3{-}4(Ti_{1-2x}{}^{4+}, Mn_{2x}{}^{3+})O_{3-x} + Ti_{2x} + O_x} \quad (1)$$

Regime (II) (Mn > 43 mol%)

$$\mathrm{BaO{-}(Nd,Sm)_2O_3{-}4TiO_2 + MnCO_3 \rightarrow BaO{-}(Nd,Sm)_2O_3{-}4(Ti_{1-2x}{}^{4+}, Mn_{2x}{}^{3+})O_{3-x} + Mn\text{-}richphase} \quad (2)$$

3.2. Measurement of microwave dielectric properties

Mn-doped BNST shows a quite complex crystalline phase as mentioned in the previous section. It is of interest to understand the effect of Mn on the dielectric properties of Mn-doped BNST. Figs. 4 and 5 respectively show the variation of insulation resistance and loss tangent of Mn-doped BNST with Mn content. The loss tangent of specimens was measured at 1 MHz. Obviously, at the critical content (Mn >43 mol%), the insulation resistance of Mn-doped BNST has been significantly enhanced and the abrupt decrease in tan δ. This result strongly implied that Mn-doped BNST sintered in a reducing atmosphere is in a semi-conducting state while Mn content is less than 42 mol% and it is in an insulating state while Mn content is more than 43 mol%. Obviously, the conductivity of Mn-doped BNST is closely related to the defect chemistry of Mn-doped BNST sintered in a reducing atmosphere. As previously reported, when $BaTiO_3$ was sintered in a reducing atmosphere,

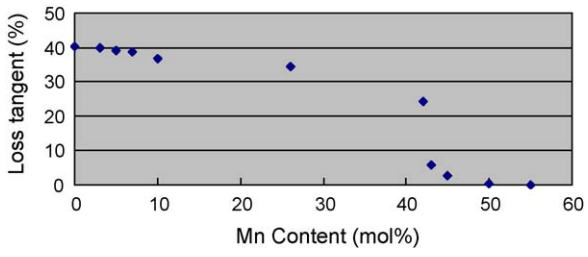

Fig. 5. Variation of tan δ as a function of Mn content.

the acceptors were often used to trap the liberation of free electron during sintering in reducing atmosphere to shift the minimum in the conductivity–oxygen pressure relation to lower oxygen pressures. As long as the number of free electrons is below that of acceptors, the material sintered in a reducing atmosphere remains in a highly insulating state. Oppositely, the material is in a semi-conducting state [9].

While Mn-doped BNST was sintered in a reducing atmosphere, it is well accepted that the mobile carrier charged species in Mn-doped BNST are oxygen vacancy ($V_O^{\bullet\bullet}$) and free electrons (e^-), which is similar to that in the case of $BaTiO_3$-based MLCC was sintered in a reducing atmosphere [10]. The reduction of oxygen simultaneously generates the higher concentration of oxygen vacancies, $V_O^{\bullet\bullet}$, and the free electrons e^-, which are mainly responsible for the movement of charged carriers under the electric field or at high temperature [11]. The oxygen removal is indicated in Eq. (3).

$$O_O \rightarrow \tfrac{1}{2}O_2(g) + V_O^{\bullet\bullet} + 2e\prime \quad (3)$$

On the other hand, Mn-doped BNST sintered in a reducing atmosphere, the generation of acceptor is from Mn incorporated into Ti-site. When Mn was doped in $BaO{-}(Nd,Sm)_2O_3{-}4TiO_4$ sintering in a reducing atmosphere and re-oxidation in N_2 atmosphere, Mn^{3+} obviously exhibits a preference for the Ti-sites. According to Eq. (4), Mn^{3+} ion doped in $BaO{-}(Nd,Sm)_2O_3{-}4TiO_4$ acts as an acceptor.

$$4MnO + 4O_2(g) \overset{BaO(Nd,Sm)_2O_3 4TiO_2}{\underset{(acceptor)}{\longrightarrow}} Ba_{Ba}^{x} + 2Re_{Re}^{x} + 4'_{Ti} + 8O_O^x + 4V_O^{\bullet\bullet} \quad (4)$$

$$Mn'_{Ti} + e\prime \rightarrow null \quad (5)$$

According to Eq. (5), the conductivity of Mn-doped BNST sintered in a reducing atmosphere is dependent on the concentration of charged carriers (acceptor; Mn'_{Ti}, and free electron; e′). Because Mn-doped BNST sintered in a reducing atmosphere is still in a semi-conducting state. This indicates that the sum of the concentration of acceptor of Mn'_{Ti} is still lower than the concentration of free electron in regime (I). However, electrical properties of Mn-doped BNST such as insulation resistance (I.R.) and tan δ can be significantly improved when the content of Mn is more than 43 mol%. The insulation resistance of Mn (>43 mol%)-doped BNST can be as high as 10^{10} Ω and the tan δ of Mn-doped BNST can be reduced below 5%. Both results indicate that the concentration of acceptor is higher than that of free electron for Mn (>43%)-doped BNST specimen. This result seems to be associated with the formation of new Mn-doped tungsten bronze-type compound. This second phase is a heavily Mn-doped (>43 mol%) into Ti-sites that provides the high concentration of acceptor, corresponding to slightly Mn-doped (<42 mol%) into Ti-sites in regime (I). Thus, Mn (>43 mol%)-doped BNST is in an insulating state.

Table 1 shows the measurement of microwave dielectric properties of Mn-doped BNST dielectrics sintered in a reducing atmosphere. The measurement of the dielectric constant is valid when the materials are in an insulating state. The dielectric

Table 1
Microwave dielectric properties of BSTN sintered in a reducing atmosphere.

Mn (mol%)	ε_r	tan $\delta \times 10^{-4}$ (MHz)	$Q \times f_o$	I.R. (Ω)	T.C.C. (ppm/°C)
0	7732	4001	–	1.87×10^{1}	–
7	7402	3860	–	3.78×10^{1}	–
26	3459	2245	–	5.53×10^{7}	–
42	242	3434	–	1.74×10^{9}	–
43	84	592	76	4.36×10^{10}	+150
44	80	449	100	7.32×10^{10}	+95
45	79	283	159	6.48×10^{10}	+37
46	75	29	1551	6.84×10^{10}	−3
47	79	27	1665	8.72×10^{10}	−30
52	84	20	2250	1.20×10^{11}	−80
55	93	16	2811	1.45×10^{11}	−125

constant of 43–55 mol% Mn-doped BNST measured at 1 MHz increases slightly with increasing the Mn content. This result is associated with that the crystalline phases of Mn-doped BNST dielectric in regime (II) consists of BaO–$(Nd,Sm)_2O_3$–$4(Ti_{1-2x}^{4+},Mn_{2x}^{3+})O_{3-x}$ and Mn-rich phase, the further increase in $MnCO_3$ content from 43 to 55 mol% may lead to the increase in the amount of Mn-rich phase that has a higher dielectric constant.

The formation of the Mn-rich second phase also affects $Q \times f_o$ factor and temperature coefficient of capacitance (T.C.C.) significantly. $Q \times f_o$ is generally affected by crystallizability, long-range ordering degree of cations and phase constitution [12,13]. When Mn content exceeds a critical value (>43 mol%), the $Q \times f_o$ factor increases continuously with increasing Mn content that is associated with the amount of the Mn-rich second phase.

The variation tendency of temperature coefficient (T.C.C.) with Mn substitution in BSTN solid solution is originated from the compensation of the opposite temperature coefficients of BaO–$(Nd,Sm)_2O_3$–$4(Ti_{1-2x}^{4+},Mn_{2x}^{3+})O_{3-x}$ and Mn-rich phase. Thus, 46 mol% Mn-doped BNST shows the promising T.C.C. characteristic (−3 ppm/°C) in this study.

4. Conclusion

For Mn-doped BNST from 0 to 55 mol% sintered in a reducing atmosphere, there are two distinguishable regimes based on their phase transformation and electrical properties.

In regime (I), Mn-doped BNST from 0 to 42 mol% sintered in a reducing atmosphere shows the crystalline phase of BaO–$(Nd,Sm)_2O_3$–$4(Ti_{1-2x}^{4+},Mn_{2x}^{3+})O_{3-x}$ (1:1:4 phase), which possesses a tungsten bronze crystal structure. Mn^{3+} incorporated into Ti^{4+}-site of BNST plays acceptor roles. However, the sum of acceptor concentration is still lower than that of the liberation of free electron from the formation of oxygen vacancies, thus, Mn (<42 mol%)-doped BNST is in a semi-conducing state.

In regime (II), Mn-doped BNST with 43–55 mol% sintered in a reducing atmosphere shows dual crystalline phases of BaO–$(Nd,Sm)_2O_3$–$4(Ti_{1-2x}^{4+},Mn_{2x}^{3+})O_{3-x}$ and the Mn-rich second phase. As the critical concentration (≥43 mol%) is reached, the electrical properties are significantly improved, especially in terms of insulation resistance and tan δ. The concentration of acceptor is higher than that of liberation of free electron. The formation of the Mn-doped tungsten bronze-type compound second phase also affects $Q \times f_o$ factor, dielectric constant and temperature coefficient of capacitance (T.C.C.) significantly.

Acknowledgement

The authors would like to acknowledge the financial support under contract No. NSC97-2216-E005-019.

References

[1] K.M. Cruickshank, X.P. Jing, G. Wood, E.E. Lachowski, A.R. West, Barium neodium titanate electroceramics: phase equilibria studies of $Ba_{6-3x}Nd_{8+2x}Ti_{18}O_{54}$ solid solution, J. Am. Ceram. Soc. 79 (6) (1996) 1605–1610.
[2] C.Y. Li, X.M. Chen, Effects of sintering conditions on microstructures and microwave dielectric properties of $Ba_{6-3x}(Sm_{1-y}Nd_y)_{8+2x}Ti_{14}O_{54}$ ceramics ($x = 2/3$), J. Eur. Ceram. Soc. 22 (2002) 715–719.
[3] N. Ichinose, H. Amada, Preparation and microwave dielectric properties of the $BaO{\cdot}(Sm_{1-x}La_x)O_3{\cdot}5TiO_2$ ceramic system, J. Eur. Ceram. Soc. 21 (2001) 2751–2753.
[4] C.A. Silva, F. Azough, R. Freer, C. Leach, Microwave dielectric ceramics in the system BaO–Li_2O–Nd_2O_3–TiO_2, J. Eur. Ceram. Soc. 20 (2000) 2727–2734.
[5] H. Kishi, Y. Okino, N. Yamaoka, Electrical properties and reliability study of multilayer ceramic capacitor with nickel electrodes, in: Proceedings of the 7th U.S., Japan Seminar on Dielectric and Piezoelectric Ceramics, 1995, p. 255.
[6] W.S. Lee, T.Y. Tseng, D. Hennings, Effects of ceramic processing parameters on the microstructure and dielectric properties of $(Ba_{1-x},Ca_x)(-)(Ti_{0.99-y},Zr_yMn_{0.01})O_3$ sintered in reducing atmosphere, J. Mater. Sci.: Mater. Electron. 12 (2001) 123–130.
[7] B.W. Hakki, P.D. Coleman, A dielectric resonator method of measuring inductive capacitance in the millimeter range, IRE Trans. Microwave Theory Technol. 8 (1960) 402–410.
[8] M.B. Varfolomeev, A.S. Mironov, V.S. Kostomarov, L.A. Golubtsova, T.A. Zolotova, The synthesis and homogeneity ranges of the phase $Ba_{6-3x}(Sm_{1-y}Nd_y)_{8+2x}Ti_{14}O_{54}$, Russ. J. Inorg. Chem. 33 (1988) 607–608.
[9] D. Kolar, S. Gaberscek, B. Volavsek, Synthesis and crystal chemistry of $BaNd_2Ti_3O_{10}$, $BaNd_2Ti_5O_{14}$ and $Nd_4Ti_9O_{24}$, J. Solid State Chem. 38 (1984) 158–164.
[10] R. Waser, T. Baiatu, K.H. Hardtl, dc electrical degradation of perovskite-type titanates I, ceramics, J. Am. Ceram. Soc. 73 (6) (1990) 1654–1662.
[11] S. Sumita, M. Lkeda, Y. Nakano, K. Nishyama, T. Nomur, Degradation of multilayer ceramic capacitor with nickel electrodes, J. Am. Ceram. Soc. 74 (11) (1991) 2739–2746.
[12] C. Grenthe, M. Sundberg, X-ray and electron microscopy studies of rare-earth tungsten bronzes, J. Solid State Chem. 167 (2002) 412–419.
[13] A.G. Belous, O.V. Ovchar, M. Valant, D. Suvorov, D. Kolar, The effect of partial isovalent substitution in the A-sublattice on MW properties of materials based on $Ba_{6-x}Ln_{8+2x/3}Ti_{14}O_{54}$ solid solutions, J. Eur. Ceram. Soc. 21 (2001) 2723–2730.